

Enhancement in NO₂ and H₂-Sensing Performance of Cu_xO/TiO₂ Nanotubes Arrays Sensors Prepared by Electrodeposition Synthesis

Araa Mebdir Holi¹✉, Ghufran Abd AL-Sajad¹, Asla Abdullah Al-Zahrani², Asmaa Soheil Najm³

¹Department of Physics, College of Education, University of Al-Qadisiyah, Al-Diwaniyah, Al-Qadisiyah 58002, Iraq.

²Imam Abdulrahman bin Faisal University, Eastern Region, Dammam, Kingdom of Saudi.

³Department of Electrical Electronic & Systems Engineering, Faculty of Engineering and Built Environment, Universiti Kebangsaan Malaysia, 43600 UKM Bangi, Selangor, Malaysia.

✉ Corresponding author. E-mail: araa.holi@qu.edu.iq

Received: Jan. 27, 2021; **Accepted:** Dec. 2, 2021; **Published:** Jan. 14, 2022

Citation: Araa Mebdir Holi, Ghufran Abd AL-Sajada, Asla Abdullah Al-Zahrani, and Asmaa Soheil Najm, Enhancement in NO₂ and H₂-Sensing Performance of Cu_xO/TiO₂ Nanotubes Arrays Sensors prepared by Electrodeposition Synthesis. *Nano Biomed. Eng.*, 2022, 14(1): 7-14.

DOI: 10.5101/nbe.v14i1.p7-14.

Abstract

The Cu_xO/TiO₂ nanotubes arrays are fabricated in two stages. Firstly, TiO₂-NTs are grown by the Ti-foil anodization process and then annealed for 2h at 500 °C. Subsequently, Cu_xO thin film was deposited with different deposition times on the nanotubes by electrochemical cathodic reaction, then heated twice, once at 200 °C in the air and then at 300 °C in the closed furnace for 2 h, respectively. Pure-TNT and Cu_xO/TNTs heterostructure are characterized by XRD, FE-SEM, EDX, Hall effect, and as a gas sensor. Results show that the gas sensor (CuO_{x=1}/TiO₂ for NO₂ and H₂ gases) prepared at the time (1 min) is higher than the pure TiO₂-NTs and also higher than Cu_{x=2}O/TiO₂ which were synthesized at various times 3, 5, 7, and 10 mins.

Keywords: Cu_xO/TiO₂ heterostructure, Gas sensor, Nanotube arrays, Electrochemical deposition

Introduction

Metal oxide (MO_x)-semiconductors are preferred materials to fabricate gas sensors due to their exceptional physical and chemical properties, low cost, and simple methods of preparation [1]. TiO₂ is one of the most commonly used n-type semiconductors among those MO_x materials [2]. Thereby TiO₂ nanotubes can be widely applied in gas sensors [3], photoelectric devices [4], photocatalytic degradation of pollutants [5], water photolysis [6]. Due to the high surface/volume ratio, expansion of the surface charge area, good chemical and thermal stability, fast response and recovery times as gas sensors, TiO₂ nanostructures

have been widely studied in the field of gas sensors over the past decades [7-9]. Nanostructures of 1D TiO₂ have been reported as a promising sensing material against H₂ [10], ethanol [11], acetone [12], CO [13], and NO₂ [14]. Because of the strong demand for better sensor properties for nearly all sensor applications, sensor technology work aims to achieve a high gas response, quick response and recovery times, and excellent selectivity sensing property, which are critical sensor parameters that need to be optimized for realistic applications [15]. Many attempts were made to integrate another material into the nanostructures of TiO₂. As well known, nanometallic oxides structures, for example, consisting of WO₃ [16], SnO₂ [17],

CuO [18], and ZnO [19] are used to form p-n or n-n junctions at the TiO₂ interface to change the band around the band, currently it turned out to be very suitable [20]. Cupric oxide or cuprite (Cu₂O), and cupric oxide or tenorite (CuO) are two common types of copper oxide [21]. CuO (monoclinic) and Cu₂O (cubic) are p-type semiconductors with a bandgap between (1.0-2.1 and 2.0-2.6) eV [22] respectively, but CuO and Cu₂O also have n-conductivity of type [23-24]. Since both materials complement each other in terms of their properties, several works have combined CuO, Cu₂O, and TiO₂ to form a new structure, TiO₂/CuO, Cu₂O, or in reverse. This research is concord on the combination of n-n type semiconductor materials to obtain better sensor output. Cu_xO/TiO₂ nanotubes (n-n) type heterostructure sensors were manufactured to investigate the effect of (n-n) type heterostructure on the sensing of NO₂ and H₂ gasses.

The TiO₂ NTs were synthesized directly on Ti foil using the anodization method. Then, Cu_xO was manufactured as n-type metaloxide by electrochemical deposition on TiO₂ NTs based on deposition time. Samples were exposed to various concentrations of NO₂ and H₂ gases at a temperature (27 °C) to investigate the sensing efficiency of the heterostructure. This is the first paper, to the best of our knowledge, on NO₂ and H₂ gas sensing by Cu_xO/TiO₂ (n-n) type heterostructure which was prepared by an electrochemical method based on deposition time.

Experimental Synthesis

Composite of Cu_xO/TiO₂ was synthesized using the following steps. In the first step, the electrochemical anodization was performed in a cell of two electrodes with the Ti foil as anode and the graphite rod as a cathode. Commercially pure titanium samples (99.999%) had dimensions (1.0×2.5) cm, followed by degreasing with ultrasonic treatment subsequently in acetone, isopropanol, and deionized DI water for 15 minutes, followed by chemical etching in 6 M HNO₃ for 10 minutes to give a fresh, smooth surface. They are then rinsed with extra deionized water and then air-dried. Both electrodes were attached to a power supply and were submerged in electrolytes consisting of 95 mL of anhydrous ethylene glycol, 5 mL of DI water, and 0.5 g of NH₄F at 40 V for 1 h. In the air atmosphere, a thermocone furnace was used to anneal the films at 500 °C with a heating rate of 2 °C/min for

2 h.

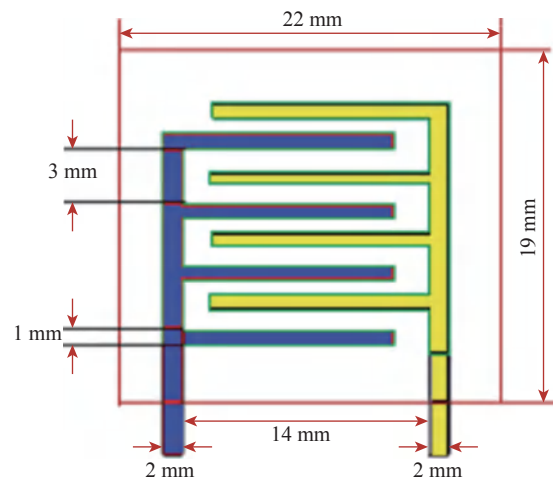
In the second step, the Cu_xO layer on top of TiO₂ NTs via electrochemical deposition was synthesized in a two-electrode cell with the TiO₂ nanotube/Ti foil as the cathode and the graphite rod as the anode. At 2 cm the distance between two electrodes was conserved. The two electrodes were connected to a power supply and they were immersed in an electrolyte consisted of anhydrous copper acetate aqueous solution (0.1 M) at 4V for 1, 3, 5, 7, and 10 min. As-prepared samples were rinsed with DI water. The samples were placed on a hot plate in the air at 200 °C for 2 h and next annealed at the temperature of 300 °C for 2 hours.

Characterization

X-ray diffraction (Shimadzu 6000 diffractometer) studied the structure and phases of the samples using CuK α radiation at 40 kV and 40 mA. Surface morphology and elemental analysis of pure TiO₂ nanotubes and Cu_xO/TiO₂ nanotubes were tested at different time deposition using SUPRA 55 VP field emission scanning electron microscope (FE-SEM) to determine film thickness, grain size, surface morphology, and cross-sectional view with 10–20 kV accelerating voltage, which is fitted with energy dispersive-ray (EDX) detectors. HMS ECOPIA 3000 (magnetic field 0.57 T, probe current 10 mA) was used to measure the electrical parameters, including carrier concentration, mobility, and resistivity.

Gas sensing measurements

The sensing measurements as illustrated in Scheme 1, were performed using two platinum pads as electrodes in the (50-300) °C temperature range. The sensing item was put in a customized chamber type



Scheme 1 Schematic description of the geometry of the electrodes.

of flow. The current was measured using a Keithley 6517A Electrometer/High Resistance Meter. The sensor temperature was monitored with a Lakeshore 340 temperature controller during the measurements. The test chamber was first purged at a steady flow rate of 100-300 ppm with high purity dry air before the current entered its stable state. The desired concentration of H_2 was obtained through a mass flow controller from the H_2 tube. For NO_2 tests a micro-syringe, containing diluted NO_2 gas was used.

Results and Discussion

Structural Characterization

XRD analysis

Fig. 1 shows XRD patterns of the TiO_2 nanotubes arrays (TNTAs) and Cu_xO/TiO_2 composite prepared at various time values scanned in the 2θ range from 20° to 70° . The peaks detected at values of 2θ correspondingly to the lattice plane as shown in Table 1. All the peaks are matched with standard indexed as tetragonal TiO_2 anatase phases (JCPDS card no. 021-1272) and TiO_2 rutile phases (JCPDS card no 021-1276) is shown in Fig. 1 TNT, while $Cu_{x=1}O$ and $Cu_{x=2}O$ thin films deposited via electrodeposition technique has a monoclinic and cubic structure, respectively.

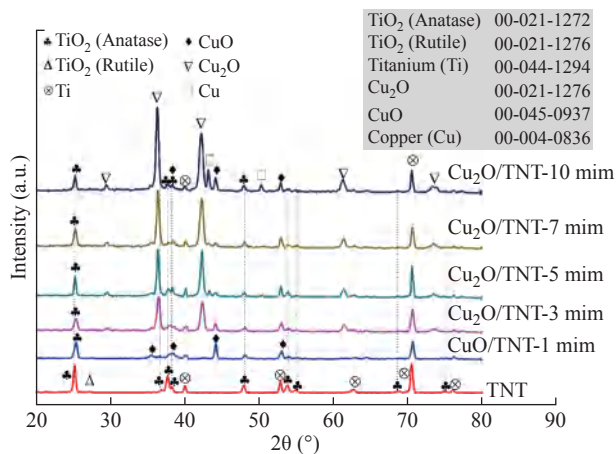


Fig. 1 XRD patterns TiO_2 TNT, CuO -1 min/TNT, Cu_2O -3 min/TNT, Cu_2O -5 min/TNT, Cu_2O -7 min/TNT, and Cu_2O -10 min/TNT.

$Cu_{x=1}O$ and $Cu_{x=2}O$ indexed (JCPDS card no. 045-0937) and (ICSD card no. 065-3288), respectively. Results show that diffraction highest peaks locating at 25.2583° , 35.549° , 36.4732° , 36.4534° , 36.6446° and 36.5465° could be observed in samples TiO_2 TNT, CuO -1 min and Cu_2O -3 min, 5 min, 7 min and, 10 min attributing to the (101), (0 0 2), (1 1 1), (1 1 1), (111) and (1 1 1) planes, respectively. When the depositing time increased from 1 min to 10 min, the intensity of the peaks increased and became sharper, this increment was obtained caused by a decrease in the crystallite size from 25.9 to 17.0 nm according to Debye-Scherrer's formula: $D = 0.9\lambda/\beta \cos \theta$.

Morphological and EDS analysis

After 60 minutes of anodization time in prepared electrolyte for Ti foil, Fig. 2(a) shows a FESEM image of pure TNTs, the surface was very filled with self-organized and well-ordered TiO_2 NTAs. The tube diameter of the samples was analyzed using image analysis software (Digimizer), the average diameter of pure TiO_2 NTs is around 70 ± 2 nm. Fig. 2(b) shows the cross-sectional image that the tubes are very smooth and aligned with the length of pure TiO_2 nanotube $\sim 2100 \pm 50$ nm. The FESEM image of the CuO/TiO_2 NTs with deposition time (1 min) is shown in Fig. 2(c). The addition of CuO results in a lower diameter of 50 ± 1 nm and reduces the aspect ratio of CuO/TNT composite tubes. The thin film CuO can be seen growing on the surface of the TNT arrays and it is apparent from the cross-sectional image view shown in Fig. 2(d) that the entire TNT including the top, inner and outer walls of the TNTs are covered in a thin film CuO with length nanotube 2400 ± 40 nm. Fig. 3 shows the EDX spectrum that demonstrated the presence of titanium, copper, and oxygen elements.

Electrical properties

Hall effect can be used to determine important parameters of the material through measurements. However, the voltage from Hall is the most important (V_H). The measurement of Hall voltage yields key

Table 1 XRD analysis for Cu_xO/TiO_2 TNT

Deposition time	2θ ($^\circ$)	FWHM (\AA)	d_{hkl} exp. (\AA)	Crys. size (nm)	d_{hkl} Std. (\AA)	[h k l]
(TiO_2) A	25.2583	0.3149	3.523532674	25.9	3.52000	[1 0 1]
CuO -1 min	35.5490	0.3149	2.523582764	26.5	2.52700	[0 0 2]
Cu_2O -3 min	36.4732	0.2952	2.461727887	28.3	2.45951	[1 1 1]
Cu_2O -5 min	36.4534	0.3739	2.463019595	22.4	2.45951	[1 1 1]
Cu_2O -7 min	36.6446	0.4330	3.011903952	19.3	2.45951	[1 1 1]
Cu_2O -10 min	36.5465	0.4920	3.013225827	17.0	2.45951	[1 1 1]

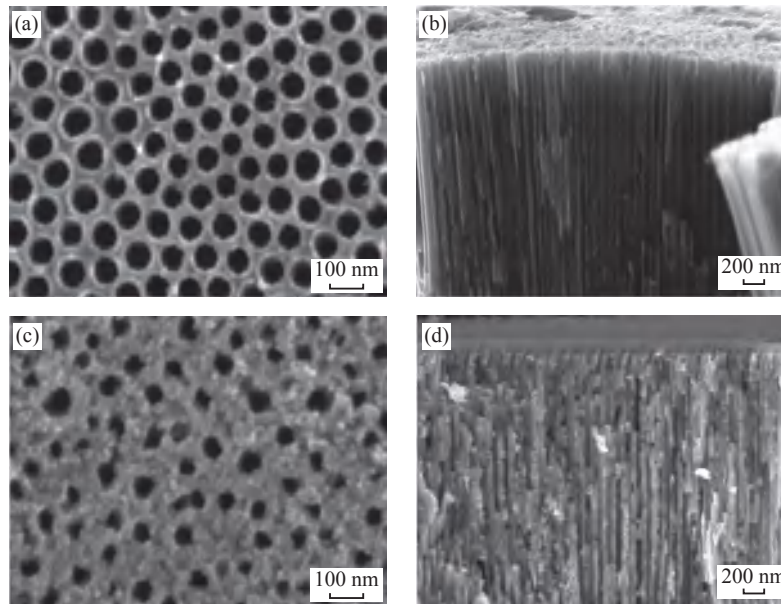


Fig. 2 FE-SEM images of the TiO_2 TNT: (a) Top view, (b) Cross-sectional, and CuO-1 min/TiO_2 TNTAs: (c) Top view, (d) Cross-sectional.

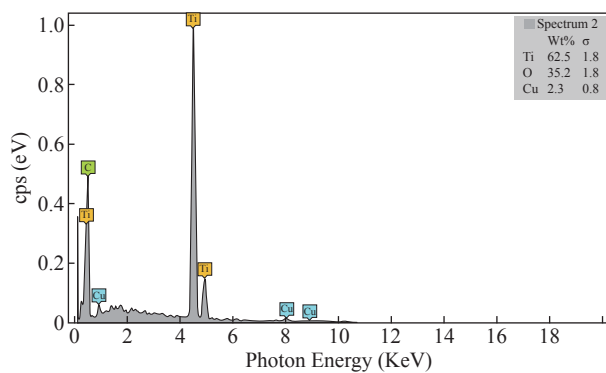


Fig. 3 The EDX spectrum of CuO-1 min/TiO_2 NTs.

characteristics such as carrier mobility (μ), carrier concentration (n), Hall coefficient (R_H), resistivity (μ), and type of conductivity (n or p).

The results obtained from the Hall effect indicated that the pure TiO_2 NTs and $\text{Cu}_x\text{O/TiO}_2$ NTs have a negative Hall coefficient (n-type). With pure TNT, conductive TiO_2 typically has carrier concentration ($-4.5 \times 10^{19} \text{ cm}^{-3}$) is higher than the reported value of electron concentration of the bare titania nanotubes that was ($-1.55 \times 10^{16} \text{ cm}^{-3}$) [25]. In literature, CuO is reported to be n-type [26-23], and sometimes p-type [9-20]. Fig. 4 shows that the carrier concentration of the composite samples $\text{Cu}_x\text{O/TNT}$ is lower than pure TNT that means the composite samples Cu_xO with TNT increase the oxygen vacancies so the number of n decreases but still n-type conductivity because of the thickness of the Cu_xO layer and the compensation effects. As known, electrons concentration determines the n-type of conductivity. It was demonstrated from Hall

measurement that the n-type conductivity behavior of Cu_xO thin films may be due to the existence of oxygen vacancies as reported by [27-30], they also used the electrodeposition method. Moreover, many researchers such as Jayakody, W. Siripala & Kumara, W. P. Siripala, and Wijesundera et al., concluded that n-type Cu_2O thin films can be synthesized on conducting substrates using the electrodeposition method [31-34]. They reported that the origin of this n-type behavior of the electrodeposited films is due to oxygen vacancies and/or additional copper atoms, and indicated that it is a consequence of strong Cu_2O absorption of an unstable surface state defective on copper formed over the p- Cu_2O surface, leading to an inversion layer that shows n-type conduction behavior [35-36]. The composite of metal-oxide- metal oxide

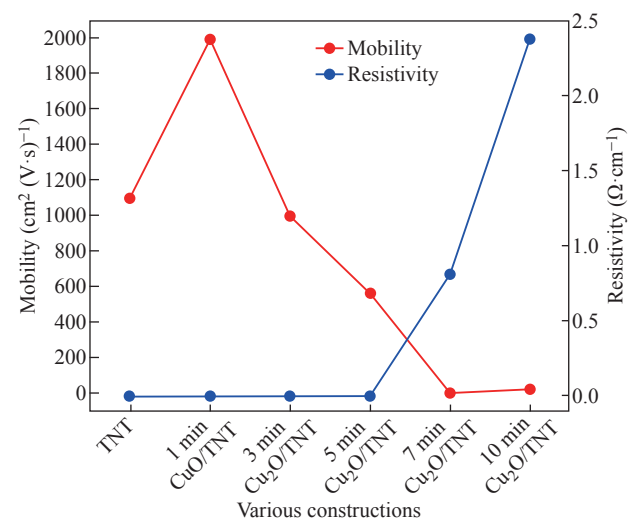


Fig. 4 Carrier concentration values of various constructions.

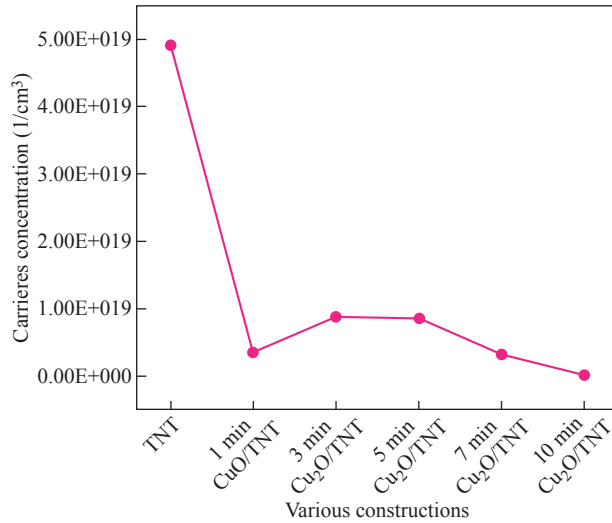


Fig. 5 Mobility and resistivity values of various constructions.

(n-n heterostructure) has a large number of defects at the heterojunction interface that may affect the type of conductivity [37]. Then, the n value increases with the increase of CuO content such behavior is expected as a result of the substitution of CuO creating one extra free carrier in the process. As the time of the deposition is increased, more aggregations occur. Thus, the resistivity increases with increasing of Cu_xO content, Fig. 5. In contrast with the Hall mobility as shown in Fig. 5, it is decreased with increasing of thickness of Cu_xO. The decrease in mobility has come from

the inverse relation between μ_H and n. This is typical of many polycrystalline thin films and is due to the existence of potential barriers in the grain boundaries [26].

Sensing properties

The response times of the Cu_xO decorated TiO₂ nanotube (NO₂ and H₂ gases) were less compared to the bare TNT sensor that can be seen in Fig. 6(a) and (b). The response times calculated for CuO-1 min/TNT sensor at (100-300) ppm of NO₂ and (100-250) ppm of H₂ at ambient temperature had improved, can be attributed to the formation of multiple (n-n) junctions at the CuO and TiO₂ interfaces. Although the heterojunction sensor's response time was increased the recovery time for both the sensors (pure sensor and heterojunction sensor) remained lower than the response times as observed in Fig. 6(c) and (d). This may be due to the low desorption rate of NO₂ and H₂ at room temperature (27 °C) [38-40].

Fig. 7(a) demonstrates the difference in sensor responses to 100 ppm of NO₂ and H₂ gas concentration for a period of 1 min of the pure TiO₂ nanotubes as a function of operating temperature from (50-300) °C. The TiO₂ nanotubes show a gradual rise in gas response and reached maximum value for NO₂ and H₂

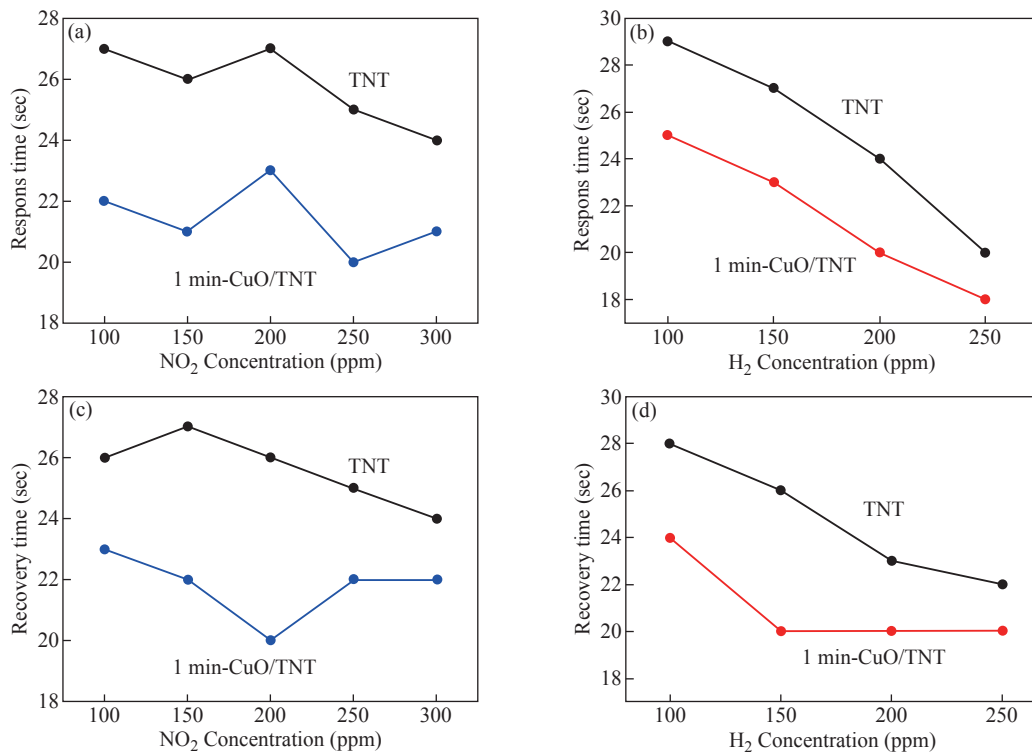


Fig. 6 Response and recovery times of the pure TiO₂ nanotubes and CuO-1 min/TiO₂ NTs heterojunction sensor calculated for (a) NO₂ and (b) H₂ at different concentrations at room temperature (27 °C).

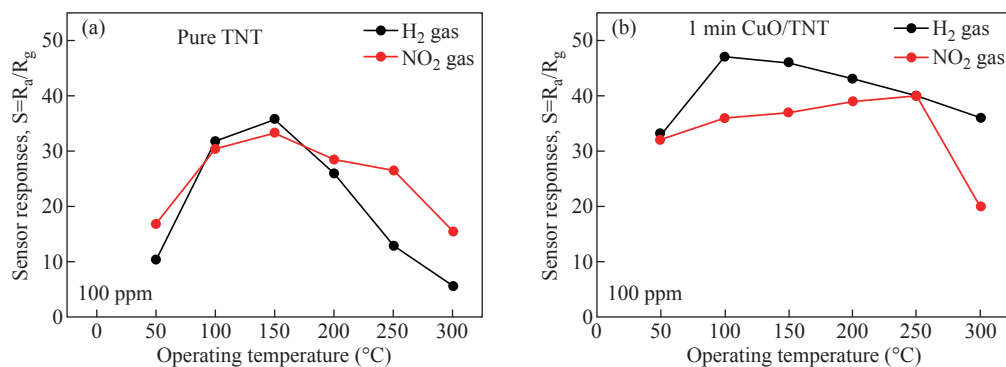


Fig. 7 Sensor responses of the device upon exposure to 100 ppm H₂ and NO₂ at different operating temperatures: (a) Pure TiO₂ NTs; (b) CuO-1 min/TNT.

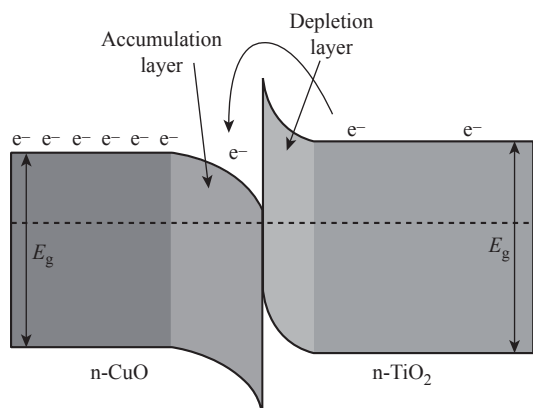
gasses at 150 °C before decreasing. The gas response of TiO₂ towards NO₂ and H₂ was decreased at operating temperatures above 150 °C. The reduction of gas exposure at higher temperatures is due to the reduction of the adsorbed NO₂ and H₂ gasses on the TiO₂ surface [10]; [41-42].

Fig. 7(b) shows that the relatively high response of CuO-1 min/TiO₂ to H₂ can be attributed to the unique hierarchical morphology of nanotubes decorated with CuO nanoparticles, which promotes the adsorption of hydrogen and oxygen surface reaction [10, 43].

Mostly on the thin film surface, H₂ molecules are adsorbed as protons and then desorbed as water vapor [44], and re-interact as hydroxyl ions with the surface. As known, when the sensor is under the reducing gas effect, the electrons obtained from the chemical reaction in the adsorbed oxygen ion forming process are given back to the conduction band. Since reduced gas acts as electron donors when interacting with the metal oxide surface, the gas desorbs or eliminates chemisorbed oxygen ions and physisorbed hydroxyl ions from the metal oxide surface during this interaction. In addition, the improved H₂ response of CuO-1 min/TiO₂ can result from the complementary contributions based on two factors. First, the enhanced adsorption of O₂ due to the TNT decoration Cu_{x=1}O shown by XRD in Fig. 1 and FESEM image Fig. 2(b) and (c) proposed a generation of more active material surface sites, which would support the gas-surface reactions. Secondly, the nanocomposite Cu_xO/TiO₂ NTs will be indeed n-n heterojunctions. Previous work has shown that TiO₂ (~2.3 eV) has a greater bandgap than Cu_{x=1}O (~2.17 eV); [45] and both conductive (C.B) and valance (V.B) bands of TNT are higher than Cu_{x=1}O, resulting in the transfer of electrons from the TiO₂ conductive band to Cu_{x=1}O [46-47]. Platinum electrode is another element that can play a role in the sensitivity

to hydrogen. Platinum can act as a catalyst for the hydrogen-titania interaction. Hydrogen dissociation on platinum surfaces can occur at elevated temperatures [10]. Results of the gas sensing test indicate that the Cu_{x=1}O loading achieved a significantly greater response better to H₂ as well as shorter response time. Whereas, the CuO-1 min/TiO₂ sensor displayed a response as high as 49% to 100 ppm H₂ at 100 °C while pure TNT was 35% at 150 °C. The efficient gas-sensing performance of the composite CuO/TiO₂ can mostly be caused by the very well-organized nanotubes morphology with heterojunction formation at the Cu_{x=1}O and TiO₂ interfaces. Fig. 7(b) also shows the CuO-1 min/TiO₂ response of NO₂ gas at 100 ppm concentration for different operating temperatures. The CuO-1 min/TiO₂ sensor exhibited a response as high as 40% toward 100-ppm NO₂ at 250 °C however as pure TNT 25% at 150 °C. The NO₂ gas interacts with the surface of a CuO-1 min/TiO₂ through surface-adsorbed NO₂ ions, which affects the number of charge carriers in the area adjacent to the surface, thus increasing the potential barrier at grain boundaries [3].

As the heterostructured CuO-1 min/TiO₂ has oxygen vacancies more than pure TiO₂ NTs that caused an increase in sensor response. The growing resistance informs us that this sensor layer is getting impoverished in the number of electrons, in resent of which the adsorbed gas molecules are forming traps localized in the forbidden band of the semiconductor. The interface at a p-n junction has far fewer free electrons, while at an interface of n-n junction simply moves electrons into the lower-energy conductive band, creating an “accumulation layer” in the Cu_{x=1}O rather than a depletion layer in TiO₂ NTs, as shown in Scheme 2. The accumulation layer may be depleted by subsequent gas adsorption on the Cu_{x=1}O surface, further enhancing the potential energy barrier at the



Scheme 2 Schematic illustration of the energy band structure at heterojunction interface of n-n type.

interface, and improving the response. The effect of heterojunction on gas sensing properties has been studied in the literature. Alev et al. studied sensing properties of copper oxide thin film/TiO₂ nanotubes heterojunction composite [18]. They reported that the improved H₂ performance of the sensor can be attributed to the heterojunction. Moreover, CuO/TiO₂ heterostructures were synthesized by Rydosz et al. for gas sensing applications [20]. They found that doping CuO into TiO₂ affects sensor performance and that the sensors are sensitive to NO₂ and H₂.

Conclusions

An anodization method was used to synthesize strongly ordered TiO₂ nanotube arrays. The nanotubes were decorated with Cu_xO nanoparticles using the electrodeposition process. Results of the gas sensing test indicate that CuO-1 min loading achieved a significantly larger response to H₂ and NO₂ as well as a shorter response time. The CuO-1 min/TiO₂ sensor showed a response as high as 49% to 100 ppm H₂ at 100 °C and 40% to 250 °C. NO₂ at 100 ppm. The excellent efficiency of the nanocomposite of gas detection can be attributed primarily to the highly ordered nanotube morphology and heterojunction at the CuO-1 min/TiO₂ interface. This paper provides the possibility of study the oxidizing and reducing gases by monitoring the response and recovery time at the different concentrations of both NO₂ and H₂ gasses and operating temperature at fixed concentration 100 ppm of NO₂ and H₂ gases for 1 minute, although further studies on these effects we are needed more investigated.

Acknowledgments

The research work presented here is supported

by the University of Al-Qadisiyah, Iraq, and Imam Abdulrahman bin Faisal University, Saudi Arabia.

Conflict of Interests

The authors declare that no competing interest exists.

References

- [1] H.W.Z.Y.L. Ji, Gas Sensing Mechanisms of Metal Oxide Semiconductors: A focus Review. *Nanoscale*, 2019, 11: 22664-22684.
- [2] G. Eranna, B.C. Joshi, D.P. Runthala, et al., Oxide materials for development of integrated gas sensors — a comprehensive review. *Critical Reviews in Solid State and Materials Sciences*, 2004, 29(3-4): 111-188.
- [3] T. Pustelny, M. Procek, E. Maciak, et al., Gas sensors based on nanostructures of semiconductors ZnO and TiO₂. *Bulletin of the Polish Academy of Sciences: Technical Sciences*, 2012, 60(4): 853-859.
- [4] A. Bally, Electronic properties of nanocrystalline titanium dioxide thin films. PhD. thesis, Ecole Polytechnique Fédéral de Lausanne (EPFL), 1999.
- [5] C.L. Chen, C.L. Dong, C.H. Chen, et al., Electronic properties of free-standing TiO₂ nanotube arrays fabricated by electrochemical anodization. *Physical Chemistry Chemical Physics*, 2015, 17(34): 22064-22071.
- [6] C. Ruan, M. Paulose, O.K. Varghese, et al., Fabrication of highly ordered TiO₂ nanotube arrays using an organic electrolyte. *Journal of Physical Chemistry B*, 2005, 109(33): 15754-15759.
- [7] X. Tong, W. Shen, X. Chen, et al., A fast response and recovery H₂S gas sensor based on free-standing TiO₂ nanotube array films prepared by one-step anodization method. *Ceramics International*, 2017, 43(16): 14200-14209.
- [8] Y.H. Chang, C.M. Liu, C. Chen, et al., The effect of geometric structure on photoluminescence characteristics of 1-D TiO₂ nanotubes and 2-D TiO₂ films fabricated by atomic layer deposition. *Journal of the Electrochemical Society*, 2012, 159(7): D401.
- [9] W. Maziarz, TiO₂/SnO₂ and TiO₂/CuO thin film nano-heterostructures as gas sensors. *Applied Surface Science*, 2019, 480: 361-370.
- [10] O.K. Varghese, D. Gong, M. Paulose, Hydrogen sensing using titania nanotubes. *Sensors and Actuators, B: Chemical*, 2003, 93(1-3): 338-344.
- [11] Y. Kwon, H. Kim, S. Lee, et al., Enhanced ethanol sensing properties of TiO₂ nanotube sensors. *Sensors and Actuators, B: Chemical*, 2012, 173: 441-446.
- [12] V. Galstyan, E. Comini, C. Baratto, et al., Two-phase titania nanotubes for gas sensing. *Procedia Engineering*, 2014, 87: 176-179.
- [13] L. Hou, C. Zhang, L. Li, et al., CO gas sensors based on p-type CuO nanotubes and CuO nanocubes: Morphology and surface structure effects on the sensing performance. *Talanta*, 2018, 188: 41-49.
- [14] T. Xie, N. Sullivan, K. Steffens, et al., UV-assisted room-temperature chemiresistive NO₂ sensor based on TiO₂ thin film. *Journal of Alloys and Compounds*, 2015, 653(2): 255-259.
- [15] J. Lee, J. Kim, and S.S. Kim, CuO-TiO₂ p-n core-shell nanowires: Sensing mechanism and p/n sensing-type transition. *Applied Surface Science*, 2018, 448: 489-497.
- [16] G.N. Chaudhari, A.M. Bende, A.B. Bodade, et al.,

- Structural and gas sensing properties of nanocrystalline TiO₂:WO₃-based hydrogen sensors. *Sensors and Actuators B: Chemical*, 2006, 115(1): 297-302.
- [17] Z. Wen, L. Tian-Mo, Gas-sensing properties of SnO₂-TiO₂-based sensor for volatile organic compound gas and its sensing mechanism. *Physica B: Condensed Matter*, 2010, 405(5): 1345-1348.
- [18] O. Alev, E. Şennik, and Z.Z. Öztürk, Improved gas sensing performance of p-copper oxide thin film/n-TiO₂ nanotubes heterostructure. *Journal of Alloys and Compounds*, 2018, 749: 221-228.
- [19] N.K. Pandey, K. Tiwari, and A. Roy, ZnO-TiO₂ nanocomposite: Characterization and moisture sensing studies. *Bulletin of Materials Science*, 2012, 35(3): 347-352.
- [20] A. Rydosz, A. Czaplá, CuO and CuO/TiO₂-y thin-film gas sensors of H₂ and NO₂. Proceedings of 2018 XV International Scientific Conference on Optoelectronic and Electronic Sensors (COE). Warsaw, Poland, Jun. 17-20, 2018.
- [21] V. Figueiredo, E. Elangovan, and G. Gonc, Effect of post-annealing on the properties of copper oxide thin films obtained from the oxidation of evaporated metallic copper. *Applied Surface Science*, 2008, 254: 3949-3954.
- [22] P. Sawicka-Chudy, M. Sibiński, E. Rybak-Wilusz, et al., Review of the development of copper oxides with titanium dioxide thin-film solar cells. *AIP Advances*, 2020, 10(1): 010701.
- [23] G. Korotcenkov, Metal oxides for solid-state gas sensors: What determines our choice? *Materials Science and Engineering B: Solid-State Materials for Advanced Technology*, 2007, 139(1): 1-23.
- [24] N. Bandara, C. Jayathilaka, D. Dissanayaka, et al., Temperature effects on gas sensing properties of electrodeposited chlorine doped and undoped n-type cuprous oxide thin films. *Journal of sensor Technology*, 2014, 4(03): 119.
- [25] R. Boddula, M.I. Ahamed, and A.M. Asiri, *Inorganic nanomaterials for supercapacitor design*. CRC Press, 2019.
- [26] S.N. Mazhir, N.H. Harb, Influence of concentration on the structural, optical and electrical properties of TiO₂:CuO thin film Fabricate by PLD. *IOSR Journal of Applied Physics*, 2015, 7(6): 14-21.
- [27] D.O. Scanlon, G.W. Watson, Undoped n-type Cu₂O: fact or fiction? *The Journal of Physical Chemistry Letters*, 2010, 1(17): 2582-2585.
- [28] X. Han, K. Han, and M. Tao, Characterization of Cl-doped n-type Cu₂O prepared by electrodeposition. *Thin Solid Films*, 2010, 518(19): 5363-5367.
- [29] L. Xiong, S. Huang, X. Yang, et al., P-Type and n-type Cu₂O semiconductor thin films: Controllable preparation by simple solvothermal method and photoelectrochemical properties. *Electrochimica Acta*, 2011, 56(6): 2735-2739.
- [30] P. Grez, F. Herrera, G. Riveros, et al., Morphological, structural, and photoelectrochemical characterization of n-type Cu₂O thin films obtained by electrodeposition. *Physica Status Solidi (a)*, 2012, 209(12): 2470-2475.
- [31] W.J.R.P.J. Siripala, J.R.P. Jayakody, Observation of n-type photoconductivity in electrodeposited copper oxide film electrodes in a photoelectrochemical cell. *Solar Energy Materials*, 1986, 14(1): 23-27.
- [32] W.P. Siripala, K.P. Kumara, A photoelectrochemical investigation of the n- and p-type semiconducting behaviour of copper(I) oxide films. *Semiconductor Science and Technology*, 1989, 4(6), 465-468.
- [33] W.P. Siripala, Electrodeposition of n-type cuprous oxide thin films. *ECS Transactions*, 2008, 11(9): 1.
- [34] R.P. Wijesundera, M. Hidaka, K. Koga, et al., Growth and characterisation of potentiostatically electrodeposited Cu₂O and Cu thin films. *Thin Solid Films*, 2006, 500(1-2): 241-246.
- [35] J.N. Nian, C.C. Tsai, P.C., Lin, et al., Elucidating the Conductivity-Type Transition Mechanism of p-Type Cu₂O Films from Electrodeposition. *Journal of The Electrochemical Society*, 2009, 156(7): H567.
- [36] D.O. Scanlon, G.W. Watson, Undoped n-type Cu₂O: Fact or fiction? *Journal of Physical Chemistry Letters*, 2010, 1(17): 2582-2585.
- [37] P. Sawicka-Chudy, G. Wisz, M. Sibiński, et al., Optical and structural properties of Cu₂O thin film as active layer in solar cells prepared by DC reactive magnetron sputtering. *Archives of Metallurgy and Materials*, 2019, 64(1): 243-250.
- [38] P. Shankar, J.B.B. Rayappan, Gas sensing mechanism of metal oxides: The role of ambient atmosphere, type of semiconductor and gases-A review. *Sci. Lett. J*, 2015, 4(4): 126.
- [39] P.P. Subha, L.S. Vikas, and M.K. Jayaraj, Solution-processed CuO/TiO₂ heterojunction for enhanced room temperature ethanol sensing applications. *Physica Scripta*, 2018, 93(5): 55001.
- [40] M. Batzill, Surface science studies of gas sensing materials: SnO₂. *Sensors*, 2006, 6(10): 1345-1366.
- [41] J. Esmaeilzadeh, E. Marzbanrad, C. Zamani, et al., Fabrication of undoped-TiO₂ nanostructure-based NO₂ high temperature gas sensor using low frequency AC electrophoretic deposition method. *Sensors and Actuators, B: Chemical*, 2012, 161(1): 401-405.
- [42] V.L. Patil, S.A. Vanalakar, S.S. Shendage, et al., Fabrication of nanogranular TiO₂ thin films by SILAR technique: Application for NO₂ gas sensor. *Inorganic and Nano-Metal Chemistry*, 2019, 49(7): 191-197.
- [43] A.Z. Sadek, J.G. Partridge, D.G. McCulloch, et al., Nanoporous TiO₂ thin film based conductometric H₂ sensor. *Thin Solid Films Nanoporous TiO₂*, 2009, 518(4): 1294-1298.
- [44] O. Wurzinger, G. Reinhardt, CO-sensing properties of doped SnO₂ sensors in H₂-rich gases. *Sensors and Actuators, B: Chemical*, 2004, 103(1-2): 104-110.
- [45] M. Ichimura, Y. Kato, Fabrication of TiO₂/Cu₂O heterojunction solar cells by electrophoretic deposition and electrodeposition. *Materials Science in Semiconductor Processing*, 2013, 16(6): 1538-1541.
- [46] Y. Li, X. Yu, and Q. Yang, Fabrication of TiO₂ nanotube thin films and their gas sensing properties. *Journal of Sensors*, 2009.
- [47] S. Ng, P. Kuberský, M. Krbal, et al., ZnO Coated Anodic 1D TiO₂ Nanotube Layers: Efficient Photo-Electrochemical and Gas Sensing Heterojunction. *Advanced Engineering Materials*, 2018, 20(2): 1-10.

Copyright© Araa Mebdir Holi, Ghufuran Abd AL-Sajada, Asla Abdullah Al-Zahrani, and Asmaa Soheil Najm. This is an open-access article distributed under the terms of the Creative Commons Attribution License, which permits unrestricted use, distribution, and reproduction in any medium, provided the original author and source are credited.